EUROPEAN RESPIRATORY *journal*

FLAGSHIP SCIENTIFIC JOURNAL OF ERS

Early View

Original article

Excess mucus viscosity and airway dehydration impact COPD airway clearance

Vivian Y. Lin, Niroop Kaza, Susan E. Birket, Harrison Kim, Lloyd J. Edwards, Jennifer LaFontaine, Linbo Liu, Marina Mazur, Stephen A. Byzek, Justin Hanes, Guillermo J. Tearney, S. Vamsee Raju, Steven M. Rowe

Please cite this article as: Lin VY, Kaza N, Birket SE, *et al*. Excess mucus viscosity and airway dehydration impact COPD airway clearance. *Eur Respir J* 2019; in press (https://doi.org/10.1183/13993003.00419-2019).

This manuscript has recently been accepted for publication in the *European Respiratory Journal*. It is published here in its accepted form prior to copyediting and typesetting by our production team. After these production processes are complete and the authors have approved the resulting proofs, the article will move to the latest issue of the ERJ online.

Excess mucus viscosity and airway dehydration impact COPD airway clearance

Vivian Y. Lin[1], Niroop Kaza[1], Susan E. Birket[1,2], Harrison Kim[3], Lloyd J. Edwards[4], Jennifer LaFontaine[2], Linbo Liu[2], Marina Mazur[2], Stephen A. Byzek[2], Justin Hanes[5], Guillermo J. Tearney[6], S. Vamsee Raju[1,2], Steven M. Rowe[1,2,*]

[1]Department of Medicine, [2]Cystic Fibrosis Research Center, [3]Department of Radiology, [4] Department of Biostatistics, University of Alabama at Birmingham, Birmingham, AL/USA.
[5]The Center for Nanomedicine at Wilmer Eye Institute, Johns Hopkins University, MD/USA.
[6]Wellman Center for Photomedicine, Massachusetts General Hospital, Boston, MA/USA.

AUTHOR CONTRIBUTIONS
V.Y.L. performed rheologic measurement of mucus samples, and analyzed the data. V.Y.L. and S.E.B. optimized the tracheal explant imaging protocol, performed µOCT imaging of airway samples, and analyzed the data. S.V.R. and H.K. performed *in vivo* MCC assays and analyzed the resulting images. S.A.B. performed *in vivo* smoke exposures. S.V.R., S.A.B., and N.K. performed animal necropsies for trachea studies. L.J.E. performed statistical modeling of µOCT data. J.F. performed histologic analysis of bronchial and lung tissue. S.A.B. measured TPM output throughout exposure studies. M.M. harvested and grew cells from human donor tissue for primary cell culture. J.H. provided fluorescent nanoparticles and expertise for particle tracking experiments. G.J.T. developed µOCT technology and all related analytical methods, and provided technical support and expertise. V.Y.L., S.E.B., S.V.R., and S.M.R. contributed to experimental design and data interpretation. V.Y.L. and S.M.R. wrote the manuscript, which was reviewed by N.K., S.E.B., S.V.R., H.K., M.M., L.P.T., S.A.B., J.H., and G.J.T.

SOURCES OF SUPPORT
This study was financially supported by the National Institutes of Health (NIH grants P30DK072482, R35HL135816, and F31HL134225), and the Flight Attendant Medical Research Institute.

RUNNING TITLE
Mucus abnormalities impact COPD airway clearance

ADDRESS FOR CORRESPONDENCE –
Steven M. Rowe, MD, MSPH
1918 University Blvd. MCLM 702
Birmingham, AL 35294
srowe@uabmc.edu
Phone: 205-934-9640

ABSTRACT

The mechanisms by which cigarette smoking impairs airway mucus clearance are not well understood. We recently established a ferret model of cigarette smoke-induced chronic obstructive pulmonary disease (COPD) exhibiting chronic bronchitis. We investigated the effects of cigarette smoke on mucociliary transport (MCT).

Adult ferrets were exposed to cigarette smoke for 6 months, with *in vivo* mucociliary clearance (MCC) measured by Tc-labeled DTPA (Tc-DTPA) retention. Excised tracheae were imaged with micro-optical coherence tomography. Mucus changes in primary human airway epithelial cells and *ex vivo* ferret airways were assessed by histology and particle tracking microrheology. Linear mixed models for repeated measures identified key determinants of MCT.

Compared to air controls, cigarette smoke-exposed ferrets exhibited mucus hypersecretion, delayed MCC (-89.0%, $P<0.01$), and impaired tracheal MCT (-29.4%, $P<0.05$). Cholinergic stimulus augmented airway surface liquid (ASL) depth (5.8±0.3 to 7.3±0.6 µm, $P<0.0001$) and restored MCT (6.8±0.8 to 12.9±1.2 mm/min, $P<0.0001$). Mixed model analysis controlling for covariates indicated smoking exposure, mucus hydration (ASL) and CBF were important predictors of MCT. Ferret mucus was hyperviscous following smoke exposure in vivo or in vitro and contributed to diminished MCT. Primary cells from smokers with and without COPD recapitulated these findings, which persisted despite the absence of continued smoke exposure.

Cigarette smoke impairs MCT by inducing airway dehydration and increased mucus viscosity, and can be partially abrogated by cholinergic secretion of fluid secretion. These data elucidate the detrimental effects of cigarette smoke exposure on mucus clearance and suggest additional avenues for therapeutic intervention.

ABSTRACT TOTAL WORD COUNT: 244/250

KEY WORDS: cigarette smoking, chronic bronchitis, mucociliary transport, mucus clearance, airway mucociliary clearance

Introduction

Chronic obstructive pulmonary disease (COPD) is the third leading cause of death in the U.S. and is increasing in incidence worldwide [1]. Although the primary risk factor is cigarette smoking [2], pathogenesis continues after smoking cessation [3], and environmental exposures or genetics can cause COPD in non-smokers [2, 4, 5].

Individuals with chronic bronchitis exhibit mucus expectoration, airway inflammation [6], and delayed mucus clearance [7, 8]. The underlying mechanisms are not yet elucidated, though mucus hypersecretion [9, 10], airway dehydration [11, 12], and rheological alterations [13] are postulated to cause muco-obstruction. Mucin hyperconcentration associated with disease severity might also underlie obstruction and exacerbations [14, 15]. Understanding their contributions will facilitate targeting these pathways for novel interventions.

We recently developed a COPD ferret model [16], which offers several advantages over traditional rodent models. For instance, ferret airways better approximate human goblet cell and glandular distribution [17, 18], yielding a mucus phenotype that includes chronic bronchitis and risk of spontaneous respiratory exacerbations, features that smoke-exposed mice lack [19, 20]. Coupling co-localized estimates of airway epithelial function [21] with mucus measurements, we can assess mucociliary transport (MCT) abnormalities and contributing physiological mechanisms not feasible in humans.

Here, we hypothesized that chronic cigarette smoke impairs the MCT apparatus by affecting mucus hydration and viscosity, and is important in slowing mucus clearance in COPD. To accomplish this, we assessed smoke-induced defects in the airway

functional microanatomy, identifying factors that determine mucus transport in a faithful model of chronic bronchitis pathogenesis.

Methods

Study approval. The University of the Alabama at Birmingham (UAB) Institutional Animal Care and Use Committee reviewed and approved animal studies (IACUC-20232, -20073, and -20232), and Institutional Review Board approved human tissue use (IRB-160901001 and -101111015). All subjects provided written informed consent for use of cells and tissues.

Cell culture. Primary human bronchial epithelial (HBE) cells were isolated from tissue from normal (non-smoker), healthy smoker (lacking lung disease), and COPD donors of varying sex, race, and age, then cultured at air-liquid interface until fully differentiated [22, 23].

Smoke exposure. Age- and gender-matched wild-type ferrets (Marshall BioResources, North Rose, NY) were exposed to room air or nose-only smoke (5 hr/day, 5 days/week, 6 months) generated by automated systems as previously described [16].

In vivo mucociliary clearance (MCC). Anesthetized ferrets were intubated (2.5 mm intra-tracheal tube extending 12 cm) and received aerosols of Tc-DTPA (upto 50 mCi / kg body weight) generated by a Raindrop Nebulizer (Aeroneb) in a safety hood that allows the ventilation of radioactive materials. Ferrets inhaled the radiolabeled aerosols generated from in 1 mL diluted in saline in 5 min. A gamma camera (Gamma Medica-Ideas, Northridge, CA) was used to measure the clearance of Tc-DTPA from both the lungs for the next 60 min. Measures of time-dependent clearance were obtained from

the entire lungs demarked with parallel CT imaging. External radiolabeled markers were placed on the ferret to facilitate proper alignment under the gamma camera and to account for decay.

The rate of mucociliary clearance was corrected for decay and expressed as percentage of radioactivity present in the initial baseline image after normalizing for systemic absorption of DTPA. The measurement of MCC was based on modifications to a previously published method involving that showed elimination kinetics of In-DTPA represent the combination of MCC and absorptive clearance [24]. Absorptive clearance of Tc-DTPA by monitoring its uptake into arm muscles (bi and tri). MCC was calculated by subtracting absorptive clearance from total clearance.

Micro-optical coherence tomography (µOCT). µOCT-recorded images of normal HBE cells and excised ferret trachea were analyzed using ImageJ (NIH, Bethesda, MD) and MATLAB software (MathWorks, Natick, MA, USA) to assess airway epithelial function [21]. Tissues were maintained on gauze saturated in warmed DMEM (Gibco, Waltham, MA, USA) containing 1 µM indomethacin (to inhibit prostaglandin signaling) [25] for images recorded immediately following excision. This was replaced with indomethacin and carbachol (1 µM each, 30 min; Sigma-Aldrich, St. Louis, MO, USA) to stimulate secretion for additional MCT measurements before mucus collection **(Fig. S2)**.

Mucus collection. Mucus was collected from unstimulated HBE cells for immediate use. Following µOCT video acquisition, ferret trachea were plugged at the ends to facilitate accumulation, then treated with 10 µM carbachol and 20 µM phenylephrine (2 hr;

Sigma-Aldrich) to maximally stimulate secretion sufficient for subsequent assays **(Fig. S2)**.

Particle tracking microrheology (PTM). Mucus samples containing fluorescent PEG-PS (500-nm or 1-µm) particles (1:10 v/v dilution) were loaded underneath a coverslip (10 µL) to assess Brownian motion of individual particles. Following 1-hr incubation, samples were imaged using µOCT or fluorescent microscopy (Nikon TE200, Nikon Instruments, Melville, NY) as previously described [26].

Mucus percent solids by weight. Aluminum foil pieces were tared on a UMX2 Ultra-microbalance (Mettler Toledo) before weighing mucus samples (5 µL HBE, 1-5 µL ferret). Samples were dried overnight (80°C) for percent non-volatile solid calculation.

Statistical analysis. All quantitative measures were analyzed using descriptive statistics and regression methods in GraphPad Prism (GraphPad Software, Inc., La Jolla, CA), SPSS Statistics (IBM, Armonk, NY), or SAS v9.4 (Cary, NC). Data are presented as mean ± standard error unless otherwise specified, with p-values < 0.05 considered statistically significant. Further details regarding methods and statistical analyses are given in the online data supplement.

Results

Mucus clearance is reduced in a ferret model of COPD.

We recently developed a cigarette smoke-induced ferret model of COPD and chronic bronchitis [16] demonstrating goblet cell hyperplasia, chronic cough, and episodic exacerbations reminiscent of human disease but not found in mouse models, providing an opportunity to identify physiological mechanisms and determine relationships to MCT apparatus abnormalities. We first measured *in vivo* mucociliary clearance (MCC) using Tc-DTPA retention **(Fig. 1A)** over time after subtracting the amount of label that eliminated via absorption; heat maps of mucociliary transport were developed to represent clearance rates. Following comparable deposition of the radiolabel in each exposure group **(Fig. S1)**, quantification of these images showed reduced clearance in smoke-exposed ferrets in 60 minutes (2.8% vs. 25.4% air controls, $P<0.01$) **(Fig. 1B).** The area under the curve (AUC) for each group demonstrated significantly higher percent retention after 60 minutes in smoke-exposed ferrets (2923±86 smoke vs. 2543±75 air control, $P<0.01$), indicating a markedly slower MCC rate compared to air controls **(Fig. 1C)**. Diminished rate of MCC was also evident, when the remaining amount of Tc-DTPA after 60 min was measured **(Fig. 1D)** despite higher clearance of the label via absorption in smoke-exposed ferrets.

Airway epithelial dysfunction impairs mucus transport in COPD.

Using µOCT analysis of excised ferret trachea **(Fig. 2A-B, S2)**, we next sought to characterize the physiologic defects within the MCT apparatus and their connections with potentially abnormal mucus. When quantified as single point estimates for

individual ferrets, there was a 29.4% reduction in MCT **(Fig. 2C)** in COPD ferrets (6.8±0.8 vs. 9.6±1.1 mm/min air controls, $P<0.05$), paralleling the reduction seen *in vivo*. A linear mixed model for repeated measures within each ferret and adjusting for two measures at baseline, cohort, and sex, confirmed the deleterious effects of smoking on MCT (32% reduction, $P=0.016$, $R^2=0.368$). Seeking potential explanations, we note that estimates by outcome were variable: both ASL **(Fig. 2D)** and PCL **(Fig. 2E)**, markers of airway hydration, exhibited small non-statistically significant reductions in cigarette smoke-exposed ferrets (by 12% and 2.9%, respectively), whereas there was no meaningful difference in CBF **(Fig. 2F)**.

To better account for the microenvironment and their interrelationships — factors known to influence each other [21, 27, 28] —we developed a statistical model that included all known covariates of MCT that were measured simultaneously and in a colocalized fashion. In preparation for this analysis, we report each individual ROI replicate in Fig. S3 by smoke exposure status. MCT was again diminished by 27.4% (mean, [95% CI]: 7.24 [6.34, 8.13] smoke vs. 9.97 [8.80, 11.14] control)) in COPD ferret airways **(Fig. S3A)**, and was also associated with a 8.8% reduction (5.91 [5.59, 6.24] smoke vs. 6.48 [6.01, 6.96] control) in ASL depth **(Fig. S3B)** and a 2.9% reduction (3.05 [2.97, 3.13] smoke vs. 3.14 [3.07, 3.21] control) in PCL depth **(Fig. S3C)** while CBF (10.63 [10.37, 10.89] smoke vs. 10.44 [10.19, 10.68] control) was relatively unchanged **(Fig. S3D)**. We then conducted univariate analysis with steady-state (pre-carbachol stimulation) MCT as the dependent variable; by ferret, reduced mean MCT was associated with smoke exposure and mean CBF **(Table S1)**. To evaluate for independent contributors to the MCT defect, we then executed a linear mixed model

that controlled for repeated measures within ferrets, but included each of the variables in the univariate analysis, in addition to experimental cohort and each of two measurements made prior to carbachol stimulation, to control for their effect (**Table 1**). Independent predictors of MCT included smoking, mean ASL depth, and mean CBF, whereas sex, baseline measurement replicate, and experimental cohort were not significant. In aggregate, these data indicate that smoking confers deleterious effects on mucus transport, and airway dehydration and ciliary dysfunction are key contributors to this dysfunction.

Assessment of primary human airway cells

We next confirmed these findings using primary HBE cells isolated from normal non-smokers and exposed to cigarette smoke, noting HBE cells do not capture the full complexity of the mucociliary transport apparatus as compared tissues such as secretion from glands. Cigarette smoke exposure reduced ASL depth **(Fig. S4A-B)**, PCL depth **(Fig. S4C)**, CBF **(Fig. S4D)** and MCT rate **(Fig. S4E)** *in vitro* using primary HBE cells imaged via µOCT, reflecting the deleterious effects of smoking on ion transport-dependent fluid secretion of airway epithelial cells [29]. Overall, our findings in primary human airway epithelial cells and a ferret model of COPD indicate chronic cigarette smoke diminishes MCT, consistent with prior observations [12, 22, 23], and does so by perturbing several aspects of the functional microanatomy.

The effect of stimulated mucus secretion

Activating glandular secretion through cholinergic stimulus can accelerate mucus transport in normal airways [30, 31], but has important deleterious effects in cystic fibrosis (CF) [28, 32, 33], inducing stasis as mucus overwhelms the ion transport apparatus, precipitating adhesive mucus, particularly at the gland duct [32, 33]. Carbachol stimulation of normal ferret trachea increased mucus fluid secretion as reflected by ASL and PCL depths (22.3% and 20.5%, P<0.0001, **Fig. 3A-B**), stimulated CBF (25.6%, P<0.0001, **Fig. 3C**), and accelerated MCT (43.0%, P<0.001, **Fig. 3D**). In contrast to CF [28, 32, 33], cholinergic stimulation of ferret trachea following smoke-induced chronic bronchitis had similar effects to that of normal trachea: carbachol significantly increased ASL depth (24.3%, P<0.05, **Fig. 3A**), PCL depth (13.0%, P<0.0001, **Fig. 3B**), CBF (25.1%, P<0.0001, **Fig. 3C**), and MCT (91.4%, P<0.0001, **Fig. 3D**) in smoke-exposed ferrets over baseline. These findings suggest that cholinergic stimulation can partially rescue defects in microanatomical function in smoking-related lung disease, where deficits in CFTR function are known to occur but not to the extent observed in CF [12, 22, 34-36].

Mucus viscosity is increased in smoke-exposed ferrets.

To determine whether smoke-exposed ferrets exhibit mucus abnormalities in the airways as observed in sputum expectorated by COPD patients [14, 37], and could contribute to effects not fully explained by airway dehydration, we performed histology on airway tissue from our ferret model, as well as particle tracking microrheology (PTM) using 500-nm particles in mucus secreted by excised trachea following stimulation (reflecting the contributions of glandular and cellular secretions, rather than mucins

adherent to the airway surface). Histologically, ferrets exposed to cigarette smoke exhibited evidence of goblet cell hyperplasia, submucosal gland hypertrophy, and overall higher amounts of mucus staining **(Fig. 4A)** – indicating a chronic bronchitis phenotype consistent with our prior report [16]. Particles in mucus from smoke-exposed ferrets obtained after carbachol stimulation (necessary to capture sufficient volume of non-adherent mucus for analysis) exhibited lower mean-squared displacement (MSD) over time **(Fig. 4B-C)** and thus, higher effective viscosity **(Fig. 4D),** including a 1.9-fold increase ($P<0.05$) at near static shear stress (0.6 Hz) **(Fig. 4E).** Solid content obtained after stimulation with carbachol demonstrated little difference (3.0±0.2% vs. 2.9±0.2% control, $P=0.32$) **(Fig. 4F)**. While initially surprising, the lack of difference in solid content indicates that the carbachol stimulation of fluid secretion was sufficient to resolve expected differences in solid content, but elevated viscosity nevertheless persisted, likely indicating the irreversibility of changes to mucus with smoke exposure, at least over short time domains evaluated in these studies.

COPD mucus is more viscous than healthy mucus.

Given that mucus viscosity and solid content have been correlated [32, 38, 39], and elevated viscosity contributes to mucus stasis in CF over and above the effects of airway dehydration alone [28, 33, 40], we next sought to establish whether viscosity played a role in human samples . We performed histology on the same tissues utilized for HBE assays, to survey differences in general appearance of the epithelium and mucus-producing structures across donor groups. Histologically, COPD and healthy smoker surface epithelia exhibited goblet cell hyperplasia and mucus impaction,

including the gland ducts, whereas each was minimal in non-smoker tissue **(Fig. 5)**. In addition, COPD tissue exhibited submucosal gland hypertrophy, and both healthy smoker and COPD glands stained more intensely with AB/PAS compared to non-smoker samples. Together, this suggests mucus is more prevalent and intensely expressed as pathology progresses to COPD.

We then analyzed viscosity of mucus derived from primary HBE cells (**Table S2**)—without pooling secretions from multiple donors, exogenous exposure to cigarette smoke, or cholinergic stimulation—by PTM **(Fig. 6A)**, noting this does not include contribution of gland mucus as the ferret samples do. MSD of 1-µm particles **(Fig. 6B)** was markedly reduced in COPD mucus compared to normal and healthy smoker donors ($P<0.05$), corresponding to significantly higher effective viscosity (**Fig. 6C**, $P<0.05$ and $P<0.01$, respectively). At 0.6 Hz **(Fig. 6D)**, mucus from COPD donors exhibited viscosity 136-fold ($p<0.01$) and 59-fold ($P<0.05$) higher than mucus from normal and healthy smokers, respectively. COPD mucus also contained significantly higher percent solids (2.77±0.15%) compared to non-smoking controls (1.57±0.05%, $P<0.0001$) and non-diseased smokers (2.01±0.05%, $P<0.0001$) **(Fig. 6E)**—findings paralleling patient sputum observations [39, 41, 42]. Healthy smoker mucus solid content was significantly higher than that of non-smoking controls ($p<0.05$), reflecting the intermediate phenotype of non-diseased smokers. Noting the absent contribution of glands in this model, we also observed that mucus solid content and effective viscosity were positively correlated ($R^2=0.7652$, $P=0.01$) **(Fig. 6F)**.

Discussion

While cigarette smoke exposure has been associated with reduced MCT and other defects of mucus *in vitro* [11, 12, 22, 23], this has never been shown in a relevant animal model, and the specific biophysical mechanisms by which smoke contributes to airway epithelial dysfunction and subsequent mucus obstruction in COPD pathogenesis remain unclear. Here, we demonstrate that cigarette smoke impairs the airway functional microanatomy in a novel COPD ferret model [16], and support findings by several complementary model systems, from *in vitro* analysis to unique assessments following *in vivo* cigarette smoke exposure. We show that diminished mucus transport is a major consequence of smoke exposure, and is impacted by airway dehydration, ciliary beating, and mucus viscosity. We further show that cholinergic stimulation of the airway epithelium can partially but not completely rescue these transport defects by augmenting fluid secretion, distinct from CF where it can worsen mucus stasis [33]. These findings implicate both airway epithelial dysfunction and mucus viscoelasticity as potential therapeutic targets for chronic bronchitis and other muco-obstructive diseases.

Our µOCT data confirm that apical cigarette smoke exposure impairs ASL and MCT *in vitro* [11, 12, 22, 23]. However, HBE cells do not fully replicate the airway surface, which contains submucosal glands. To examine this more comprehensively than is possible in cell monolayers, we employed an experimental *in vivo* model that could capture contributions of both the surface epithelium and airway glands. To this end, ferrets more closely resemble humans in terms of airway goblet cell and glandular distribution [17], and are large enough to provide an accurate representation of mucus properties. *In vivo* MCC assays demonstrated higher retention of Tc-DTPA in smoke-

exposed animals. While human studies largely rely on radiographic clearance of Tc-sulfur colloid (Tc-SC), minimal clearance occurred in ferrets due to excessive alveolar deposition, whereas Tc-DTPA nebulization distributed to the airways in sufficient quantity. Supporting our approach, multiple reports [24, 43, 44] confirm the utility of DTPA particles in distinguishing absorptive clearance from MCC if absorption can be independently estimated and accounted for, as we have done here. In addition, it has been reported that DTPA clearance by absorption is only ~50% of its total clearance [44], suggesting sufficient discrimination for estimating MCC with appropriate normalization. Inflammation reduces epithelial integrity causing increased absorption of inhaled particles [45]. Thus, our observation of greater absorption of Tc-DTPA in smoke-exposed ferret lungs when compared to control ferret lungs is consistent with what may be expected in COPD lungs with exaggerated inflammation. We find it important to note that despite increased absorptive clearance of Tc-DTPA in smoke-exposed ferrets, total amount of Tc-DTPA remaining in lungs at the end of 60 min was higher than that of controls, suggesting significantly impaired MCC. Karacavus et al. have reported that differences in MCC as a factor of current smoking status can be distinguished in control and asthma subjects using Tc-DTPA, adding further support to our approach [46].

The defect in MCC translated to impaired tracheal MCT, indicating that mucus clearance is delayed in both the upper and lower airways of our model, and that the airway surface microenvironment is important in determining mucus transport, likely due to the co-interaction of functional parameters. Although the effect of cigarette smoke was much more dramatic in MCC measurements *in vivo* compared to tracheal MCT

assessments, it should be noted that MCC estimates take into account the entire tracheobronchial tree (including smaller airways, in which mucus obstruction may occur earlier and more dramatically, or which may drop out entirely) [47], whereas *ex vivo* tracheal MCT only provides us measures in the most ciliated portion of the airways (which also contains the highest glandular and goblet cell contributions). It is also possible that cigarette smoke exposure in this model affects the whole lung more than the trachea itself, and may be dependent on dwell time in the respective regions, as well as deposition of particulate matter of various sizes. While our MCC method accounted for absorptive clearance that also occurs with DTPA, it is possible residual differences in absorption for which our calculations did not account.

Given the power of µOCT to assess covariates of the airway microanatomy simultaneously and in a co-localized manner, we used this technique to measure smoke-induced changes in excised ferret trachea, and to examine their independent contributions, controlled for multiple replicates. Specifically, we used µOCT-acquired measures to identify how individual functional parameters interact with MCT, and which are important in predicting mucus transport. As observed in other smoke exposure models, we found significant reductions in MCT (corroborating our *in vivo* MCC results) and CBF in smoke-exposed ferrets. When accounting for multiple contributors to delayed mucus clearance, mixed model analysis revealed that augmented ASL (airway hydration) and CBF (ciliary function) had positive effects on steady-state MCT, while smoke exposure had a negative impact. It should be noted that there could be other factors not easily measured in our model that may impact mucus clearance at all levels, such as ASL pH, DNA content, mucus adherence to the epithelial surface, differential

presence of specific mucins, and mucin cross-linking; these deserve further study to examine their potential. Increased mucin secretion and concentration have been suggested as another mechanism leading to thicker mucus [14, 39], and were born out by pathologic analysis of ferret tissues and the bronchi of human cell donors.

Based on the fact that MCC and MCT were clearly diminished by smoking, but deficits in CBF and airway hydration did not explain the entirety of the defect, we used microrheologic methods to assess the viscosity of normal (non-CF, non-COPD) and COPD mucus from cell monolayers and ferret tissues, since this could account for additional deficits in MCT. Similar to observations in patient sputum [37, 39], mucus collected from COPD HBE cells exhibited higher viscosity than that of non-diseased cells, even without additional cigarette smoke exposure, indicating an intrinsic defect in COPD mucus. To the best of our knowledge, this is the first evidence of increased viscosity in mucus secreted by an *in vitro* COPD model that rules out the presence of covariates unrelated to the epithelium itself, and was confirmed in samples from well-controlled ferret exposures. Additionally, COPD HBE mucus demonstrated higher percent solids by weight, which is in agreement with recent studies in normal and COPD cells [39] and sputum [14, 41]; although differences between groups were small, HBE cells lack submucosal glands, and are likely missing a significant contribution present *in vivo*. These data suggest exposure-related alterations in mucin structure or the overall mucus meshwork, potentially fruitful areas for additional research targeting correction of abnormal mucus.

Interestingly, mucus secreted by cells from healthy smokers yielded solid content and viscosity at levels intermediary to non-smoker and COPD samples, as well as

evidence of goblet cell hyperplasia and increased epithelial mucus staining. While limited by small numbers due to the availability of clinically characterized transplant specimens, this suggests that airways exposed to cigarette smoke not only produce more mucus, but it is more viscous, even without (or prior to) disease being established, and that continual and chronic exposure to high levels of inhaled irritants may increase mucus production and impair mucus clearance even in a non-pathological state. This, in addition to higher mucin concentrations observed in sputum produced by non-diseased symptomatic smokers compared to asymptomatic ones [14], may provide a significant mechanistic basis underlying mucus obstruction in COPD and could prove useful for diagnostic purposes, or even a potential prevention target should smoking cessation prove unsuccessful. This may also explain epidemiologic associations of respiratory infections with smoking [48].

Unlike observations in CF airways following cholinergic stimulation of secretion [30, 32, 33], we demonstrated cholinergic stimulus, applied from the serosal surface then allowed to equilibrate, rescued MCT defects in COPD ferret tracheae even though decrements in ASL and PCL persisted. This suggests that COPD airway epithelia have the capacity to overcome this impairment, potentially because smoke-exposed epithelia still express functional anion channels, including present but diminished CFTR, which cholinergic-stimulated Ca^{2+} release may potentially activate [49, 50]. This benefit may precede complete rehydration of airway mucus. Based on this, activating ion transport to normalize epithelial secretion or hydration represents a viable therapeutic avenue, as previously proposed to address MCT defects resulting from smoke-induced dehydration [12, 22, 23]. Anticholinergic therapies, i.e. long-acting muscarinic antagonists (LAMAs),

reduce cholinergic tone to improve airway conductance, and can also reduce mucus production; when used in conjunction with long-acting β-adrenoceptor agonists (LABAs), which may enhance ciliary beating and thus mucociliary clearance, they can lower exacerbation frequency and severity [51]. Since LAMAs are antimuscarinic agents, we speculate that compounds targeting the nicotinic arm of cholinergic pathways may also be useful, particularly since pathway disruption downstream of smoke exposure includes nicotinic receptors, and would be expected to confer distinct effects on epithelial function from that of the smooth muscle [52-54]. Given that carbachol—a non-specific cholinergic that can bind muscarinic and nicotinic receptors—increased fluid secretion as well as MCT in ferrets and in a synergistic fashion with cyclic-AMP agonists [55], this suggests that the nicotinic pathway, when targeted selectively, may be a viable and novel target to improve mucus clearance without interfering with the standard use of antimuscarinic agents to treat COPD. Future studies to assess the effects of independent activation of nicotinic and muscarinic receptors would be necessary to elucidate whether this approach is feasible without compromising the beneficial effects of anticholinergic therapy on smooth muscle tone and mucus production in these patients, much like the complementary use of LABAs. Because our findings support augmenting ion channel secretion to attenuate mucus clearance defects, activation or potentiation of CFTR itself represents an alternative approach that is currently under investigation [22, 23].

In summary, we demonstrate using several complementary models that chronic cigarette smoke exposure reduces mucociliary transport by impairing airway epithelial function (ciliary dysfunction, reduced hydration), and by altering mucus properties

(increasing solid content and viscosity). Given these findings, augmenting aspects of the airway functional microanatomy to facilitate mucus transport in chronic bronchitis may prove beneficial for improving overall mucus clearance. Due to the heterogeneity of COPD, it may be necessary to combine therapies targeting specific mechanisms underlying its pathogenesis on an individual basis to ultimately slow disease progression.

ACKNOWLEDGMENTS

The authors acknowledge A. Fulce, J. Frost-Deleersnyder, and the Tissue Collection and Banking Facility at the University of Alabama at Birmingham (UAB) for services related to airway tissue procurement and histopathology; S. Samuels and the UAB Small Animal Imaging Shared Facility for their assistance with MCC imaging; K.K. Chu and H.M. Leung (Wellman) for their maintenance of the μOCT system and expertise in developing and updating custom MatLab scripts for μOCT image analysis; and G. Duncan and S. Shenoy (Johns Hopkins) for their assistance with fluorescent particles used for PTM. The authors also thank H. Hathorne for regulatory support regarding work with human subjects and the patients who donated their organs for these experiments.

References

1. Global, regional, and national life expectancy, all-cause mortality, and cause-specific mortality for 249 causes of death, 1980-2015: a systematic analysis for the Global Burden of Disease Study 2015. *Lancet (London, England)* 2016: 388(10053): 1459-1544.
2. Mannino DM, Buist AS. Global burden of COPD: risk factors, prevalence, and future trends. *Lancet (London, England)* 2007: 370(9589): 765-773.
3. Mannino DM, Gagnon RC, Petty TL, Lydick E. Obstructive lung disease and low lung function in adults in the United States: data from the National Health and Nutrition Examination Survey, 1988-1994. *Archives of internal medicine* 2000: 160(11): 1683-1689.
4. Schikowski T, Mills IC, Anderson HR, Cohen A, Hansell A, Kauffmann F, Kramer U, Marcon A, Perez L, Sunyer J, Probst-Hensch N, Kunzli N. Ambient air pollution: a cause of COPD? *The European respiratory journal* 2014: 43(1): 250-263.
5. Salvi SS, Barnes PJ. Chronic obstructive pulmonary disease in non-smokers. *Lancet (London, England)* 2009: 374(9691): 733-743.
6. Saetta M, Turato G, Baraldo S, Zanin A, Braccioni F, Mapp CE, Maestrelli P, Cavallesco G, Papi A, Fabbri LM. Goblet cell hyperplasia and epithelial inflammation in peripheral airways of smokers with both symptoms of chronic bronchitis and chronic airflow limitation. *American journal of respiratory and critical care medicine* 2000: 161(3 Pt 1): 1016-1021.
7. Morgan L, Pearson M, de Iongh R, Mackey D, van der Wall H, Peters M, Rutland J. Scintigraphic measurement of tracheal mucus velocity in vivo. *The European respiratory journal* 2004: 23(4): 518-522.
8. Moller W, Felten K, Sommerer K, Scheuch G, Meyer G, Meyer P, Haussinger K, Kreyling WG. Deposition, retention, and translocation of ultrafine particles from the central airways and lung periphery. *American journal of respiratory and critical care medicine* 2008: 177(4): 426-432.
9. Haswell LE, Hewitt K, Thorne D, Richter A, Gaca MD. Cigarette smoke total particulate matter increases mucous secreting cell numbers in vitro: a potential model of goblet cell hyperplasia. *Toxicology in vitro : an international journal published in association with BIBRA* 2010: 24(3): 981-987.
10. Innes AL, Woodruff PG, Ferrando RE, Donnelly S, Dolganov GM, Lazarus SC, Fahy JV. Epithelial mucin stores are increased in the large airways of smokers with airflow obstruction. *Chest* 2006: 130(4): 1102-1108.
11. Clunes LA, Davies CM, Coakley RD, Aleksandrov AA, Henderson AG, Zeman KL, Worthington EN, Gentzsch M, Kreda SM, Cholon D, Bennett WD, Riordan JR, Boucher RC, Tarran R. Cigarette smoke exposure induces CFTR internalization and insolubility, leading to airway surface liquid dehydration. *FASEB journal : official publication of the Federation of American Societies for Experimental Biology* 2012: 26(2): 533-545.
12. Rasmussen JE, Sheridan JT, Polk W, Davies CM, Tarran R. Cigarette smoke-induced Ca2+ release leads to cystic fibrosis transmembrane conductance regulator (CFTR) dysfunction. *The Journal of biological chemistry* 2014: 289(11): 7671-7681.
13. Chen EY, Sun A, Chen CS, Mintz AJ, Chin WC. Nicotine alters mucin rheological properties. *American journal of physiology Lung cellular and molecular physiology* 2014: 307(2): L149-157.
14. Kesimer M, Ford AA, Ceppe A, Radicioni G, Cao R, Davis CW, Doerschuk CM, Alexis NE, Anderson WH, Henderson AG, Barr RG, Bleecker ER, Christenson SA, Cooper CB, Han MK, Hansel NN, Hastie AT, Hoffman EA, Kanner RE, Martinez F, Paine R, 3rd, Woodruff PG, O'Neal WK, Boucher RC. Airway Mucin Concentration as a Marker of Chronic Bronchitis. *The New England journal of medicine* 2017: 377(10): 911-922.

15. Livraghi-Butrico A, Grubb BR, Wilkinson KJ, Volmer AS, Burns KA, Evans CM, O'Neal WK, Boucher RC. Contribution of mucus concentration and secreted mucins Muc5ac and Muc5b to the pathogenesis of muco-obstructive lung disease. *Mucosal Immunology* 2016: 10: 395.
16. Raju SV, Kim H, Byzek SA, Tang LP, Trombley JE, Jackson P, Rasmussen L, Wells JM, Libby EF, Dohm E, Winter L, Samuel SL, Zinn KR, Blalock JE, Schoeb TR, Dransfield MT, Rowe SM. A ferret model of COPD-related chronic bronchitis. *JCI insight* 2016: 1(15): e87536.
17. Hajighasemi-Ossareh M, Borthwell RM, Lachowicz-Scroggins M, Stevens JE, Finkbeiner WE, Widdicombe JH. Distribution and size of mucous glands in the ferret tracheobronchial tree. *Anatomical record (Hoboken, NJ : 2007)* 2013: 296(11): 1768-1774.
18. Sun X, Olivier AK, Liang B, Yi Y, Sui H, Evans TI, Zhang Y, Zhou W, Tyler SR, Fisher JT, Keiser NW, Liu X, Yan Z, Song Y, Goeken JA, Kinyon JM, Fligg D, Wang X, Xie W, Lynch TJ, Kaminsky PM, Stewart ZA, Pope RM, Frana T, Meyerholz DK, Parekh K, Engelhardt JF. Lung phenotype of juvenile and adult cystic fibrosis transmembrane conductance regulator-knockout ferrets. *American journal of respiratory cell and molecular biology* 2014: 50(3): 502-512.
19. Groneberg DA, Chung KF. Models of chronic obstructive pulmonary disease. *Respiratory research* 2004: 5: 18.
20. Wright JL, Cosio M, Churg A. Animal models of chronic obstructive pulmonary disease. *American journal of physiology Lung cellular and molecular physiology* 2008: 295(1): L1-l15.
21. Liu L, Chu KK, Houser GH, Diephuis BJ, Li Y, Wilsterman EJ, Shastry S, Dierksen G, Birket SE, Mazur M, Byan-Parker S, Grizzle WE, Sorscher EJ, Rowe SM, Tearney GJ. Method for quantitative study of airway functional microanatomy using micro-optical coherence tomography. *PloS one* 2013: 8(1): e54473.
22. Sloane PA, Shastry S, Wilhelm A, Courville C, Tang LP, Backer K, Levin E, Raju SV, Li Y, Mazur M, Byan-Parker S, Grizzle W, Sorscher EJ, Dransfield MT, Rowe SM. A pharmacologic approach to acquired cystic fibrosis transmembrane conductance regulator dysfunction in smoking related lung disease. *PloS one* 2012: 7(6): e39809.
23. Raju SV, Lin VY, Liu L, McNicholas CM, Karki S, Sloane PA, Tang L, Jackson PL, Wang W, Wilson L, Macon KJ, Mazur M, Kappes JC, DeLucas LJ, Barnes S, Kirk K, Tearney GJ, Rowe SM. The Cystic Fibrosis Transmembrane Conductance Regulator Potentiator Ivacaftor Augments Mucociliary Clearance Abrogating Cystic Fibrosis Transmembrane Conductance Regulator Inhibition by Cigarette Smoke. *American journal of respiratory cell and molecular biology* 2017: 56(1): 99-108.
24. Corcoran TE, Thomas KM, Brown S, Myerburg MM, Locke LW, Pilewski JM. Liquid hyper-absorption as a cause of increased DTPA clearance in the cystic fibrosis airway. *EJNMMI Res* 2013: 3(1): 14.
25. Cho HJ, Joo NS, Wine JJ. Mucus secretion from individual submucosal glands of the ferret trachea. *American journal of physiology Lung cellular and molecular physiology* 2010: 299(1): L124-136.
26. Chu KK, Mojahed D, Fernandez CM, Li Y, Liu L, Wilsterman EJ, Diephuis B, Birket SE, Bowers H, Martin Solomon G, Schuster BS, Hanes J, Rowe SM, Tearney GJ. Particle-Tracking Microrheology Using Micro-Optical Coherence Tomography. *Biophysical journal* 2016: 111(5): 1053-1063.
27. Liu L, Shastry S, Byan-Parker S, Houser G, K KC, Birket SE, Fernandez CM, Gardecki JA, Grizzle WE, Wilsterman EJ, Sorscher EJ, Rowe SM, Tearney GJ. An autoregulatory mechanism governing mucociliary transport is sensitive to mucus load. *American journal of respiratory cell and molecular biology* 2014: 51(4): 485-493.
28. Birket SE, Chu KK, Liu L, Houser GH, Diephuis BJ, Wilsterman EJ, Dierksen G, Mazur M, Shastry S, Li Y, Watson JD, Smith AT, Schuster BS, Hanes J, Grizzle WE, Sorscher EJ,

Tearney GJ, Rowe SM. A functional anatomic defect of the cystic fibrosis airway. *American journal of respiratory and critical care medicine* 2014: 190(4): 421-432.
29. Rab A, Rowe SM, Raju SV, Bebok Z, Matalon S, Collawn JF. Cigarette smoke and CFTR: implications in the pathogenesis of COPD. *American journal of physiology Lung cellular and molecular physiology* 2013: 305(8): L530-541.
30. Ermund A, Meiss LN, Dolan B, Bahr A, Klymiuk N, Hansson GC. The mucus bundles responsible for airway cleaning are retained in cystic fibrosis and by cholinergic stimulation. *The European respiratory journal* 2018: 52(2).
31. Jeong JH, Joo NS, Hwang PH, Wine JJ. Mucociliary clearance and submucosal gland secretion in the ex vivo ferret trachea. *American journal of physiology Lung cellular and molecular physiology* 2014: 307(1): L83-93.
32. Birket SE, Davis JM, Fernandez CM, Tuggle KL, Oden AM, Chu KK, Tearney GJ, Fanucchi MV, Sorscher EJ, Rowe SM. Development of an airway mucus defect in the cystic fibrosis rat. *JCI insight* 2018: 3(1).
33. Hoegger MJ, Fischer AJ, McMenimen JD, Ostedgaard LS, Tucker AJ, Awadalla MA, Moninger TO, Michalski AS, Hoffman EA, Zabner J, Stoltz DA, Welsh MJ. Impaired mucus detachment disrupts mucociliary transport in a piglet model of cystic fibrosis. *Science (New York, NY)* 2014: 345(6198): 818-822.
34. Cantin AM, Hanrahan JW, Bilodeau G, Ellis L, Dupuis A, Liao J, Zielenski J, Durie P. Cystic fibrosis transmembrane conductance regulator function is suppressed in cigarette smokers. *American journal of respiratory and critical care medicine* 2006: 173(10): 1139-1144.
35. Raju SV, Jackson PL, Courville CA, McNicholas CM, Sloane PA, Sabbatini G, Tidwell S, Tang LP, Liu B, Fortenberry JA, Jones CW, Boydston JA, Clancy JP, Bowen LE, Accurso FJ, Blalock JE, Dransfield MT, Rowe SM. Cigarette smoke induces systemic defects in cystic fibrosis transmembrane conductance regulator function. *American journal of respiratory and critical care medicine* 2013: 188(11): 1321-1330.
36. Courville CA, Tidwell S, Liu B, Accurso FJ, Dransfield MT, Rowe SM. Acquired defects in CFTR-dependent beta-adrenergic sweat secretion in chronic obstructive pulmonary disease. *Respiratory research* 2014: 15: 25.
37. Serisier DJ, Carroll MP, Shute JK, Young SA. Macrorheology of cystic fibrosis, chronic obstructive pulmonary disease & normal sputum. *Respiratory research* 2009: 10: 63.
38. Ma JT, Tang C, Kang L, Voynow JA, Rubin BK. Cystic Fibrosis Sputum Rheology Correlates With Both Acute and Longitudinal Changes in Lung Function. *Chest* 2018.
39. Hill DB, Vasquez PA, Mellnik J, McKinley SA, Vose A, Mu F, Henderson AG, Donaldson SH, Alexis NE, Boucher RC, Forest MG. A biophysical basis for mucus solids concentration as a candidate biomarker for airways disease. *PloS one* 2014: 9(2): e87681.
40. Gustafsson JK, Ermund A, Ambort D, Johansson ME, Nilsson HE, Thorell K, Hebert H, Sjovall H, Hansson GC. Bicarbonate and functional CFTR channel are required for proper mucin secretion and link cystic fibrosis with its mucus phenotype. *The Journal of experimental medicine* 2012: 209(7): 1263-1272.
41. Anderson WH, Coakley RD, Button B, Henderson AG, Zeman KL, Alexis NE, Peden DB, Lazarowski ER, Davis CW, Bailey S, Fuller F, Almond M, Qaqish B, Bordonali E, Rubinstein M, Bennett WD, Kesimer M, Boucher RC. The Relationship of Mucus Concentration (Hydration) to Mucus Osmotic Pressure and Transport in Chronic Bronchitis. *American journal of respiratory and critical care medicine* 2015: 192(2): 182-190.
42. Lin VY, Fain MD, Jackson PL, Berryhill TF, Wilson LS, Mazur M, Barnes SJ, Blalock JE, Raju SV, Rowe SM. Vaporized E-Cigarette Liquids Induce Ion Transport Dysfunction in Airway Epithelia. *American journal of respiratory cell and molecular biology* 2018.
43. Dawkins L, Corcoran O. Acute electronic cigarette use: nicotine delivery and subjective effects in regular users. *Psychopharmacology* 2014: 231(2): 401-407.

44. Locke LW, Myerburg MM, Markovetz MR, Parker RS, Weber L, Czachowski MR, Harding TJ, Brown SL, Nero JA, Pilewski JM, Corcoran TE. Quantitative imaging of airway liquid absorption in cystic fibrosis. *Eur Respir J* 2014: 44(3): 675-684.
45. Sundram FX. Clinical studies of alveolar-capillary permeability using technetium-99m DTPA aerosol. *Ann Nucl Med* 1995: 9(4): 171-178.
46. Karacavus S, Intepe YS. The role of Tc-99m DTPA aerosol scintigraphy in the differential diagnosis of COPD and asthma. *The clinical respiratory journal* 2015: 9(2): 189-195.
47. McDonough JE, Yuan R, Suzuki M, Seyednejad N, Elliott WM, Sanchez PG, Wright AC, Gefter WB, Litzky L, Coxson HO, Pare PD, Sin DD, Pierce RA, Woods JC, McWilliams AM, Mayo JR, Lam SC, Cooper JD, Hogg JC. Small-airway obstruction and emphysema in chronic obstructive pulmonary disease. *N Engl J Med* 2011: 365(17): 1567-1575.
48. Bagaitkar J, Demuth DR, Scott DA. Tobacco use increases susceptibility to bacterial infection. *Tobacco induced diseases* 2008: 4: 12.
49. Gustafsson JK, Linden SK, Alwan AH, Scholte BJ, Hansson GC, Sjovall H. Carbachol-induced colonic mucus formation requires transport via NKCC1, K(+) channels and CFTR. *Pflugers Archiv : European journal of physiology* 2015: 467(7): 1403-1415.
50. Thiagarajah JR, Song Y, Haggie PM, Verkman AS. A small molecule CFTR inhibitor produces cystic fibrosis-like submucosal gland fluid secretions in normal airways. *FASEB journal : official publication of the Federation of American Societies for Experimental Biology* 2004: 18(7): 875-877.
51. Beeh KM, Burgel PR, Franssen FME, Lopez-Campos JL, Loukides S, Hurst JR, Flezar M, Ulrik CS, Di Marco F, Stolz D, Valipour A, Casserly B, Stallberg B, Kostikas K, Wedzicha JA. How Do Dual Long-Acting Bronchodilators Prevent Exacerbations of Chronic Obstructive Pulmonary Disease? *American journal of respiratory and critical care medicine* 2017: 196(2): 139-149.
52. Maouche K, Medjber K, Zahm JM, Delavoie F, Terryn C, Coraux C, Pons S, Cloez-Tayarani I, Maskos U, Birembaut P, Tournier JM. Contribution of alpha7 nicotinic receptor to airway epithelium dysfunction under nicotine exposure. *Proceedings of the National Academy of Sciences of the United States of America* 2013: 110(10): 4099-4104.
53. Rosas-Ballina M, Goldstein RS, Gallowitsch-Puerta M, Yang L, Valdes-Ferrer SI, Patel NB, Chavan S, Al-Abed Y, Yang H, Tracey KJ. The selective alpha7 agonist GTS-21 attenuates cytokine production in human whole blood and human monocytes activated by ligands for TLR2, TLR3, TLR4, TLR9, and RAGE. *Mol Med* 2009: 15(7-8): 195-202.
54. Galle-Treger L, Suzuki Y, Patel N, Sankaranarayanan I, Aron JL, Maazi H, Chen L, Akbari O. Nicotinic acetylcholine receptor agonist attenuates ILC2-dependent airway hyperreactivity. *Nature communications* 2016: 7: 13202.
55. Joo NS, Jeong JH, Cho HJ, Wine JJ. Marked increases in mucociliary clearance produced by synergistic secretory agonists or inhibition of the epithelial sodium channel. *Scientific reports* 2016: 6: 36806.

TABLES

Table 1. Linear mixed-effects model identifying predictors of steady-state MCT (n = 55 ferrets). $R^2 = 0.56$, $P<0.001$.

Predictor	Estimate	Standard error	P-value
Sex	-0.7922	1.1016	0.4768
Smoke	**-3.1912**	**0.9658**	**0.0022**
ASL	**-0.6433**	**0.2244**	**0.0072**
PCL	**4.0598**	**2.2289**	**0.0778**
CBF	**1.2990**	**0.4684**	**0.0085**
Baseline replicate	-0.2009	0.5696	0.7257
Cohort A	2.6826	3.2254	0.4091
Cohort B	4.0987	4.1197	0.3272
Cohort C	2.1199	3.8897	0.5892
Cohort D	7.5397	5.1513	0.1526
Cohort E	-1.2199	2.9494	0.6818
Cohort F	1.8132	3.1679	0.5711
Cohort G	4.9033	3.4162	0.1607

FIGURE LEGENDS

Figure 1. *In vivo* mucociliary clearance is impaired in a ferret model of COPD. (A) Representative images depicting percent clearance of DTPA-conjugated Tc^{99} from the lungs over time in ferrets exposed to room air or nose-only cigarette smoke for 6 months. Red = areas of maximal clearance (~2%/min). Dark blue/black = regions of minimal clearance (0%/min). **(B)** Quantification of percent clearance over time. **(C)** Area under the curve (AUC) for percent retention after 60 min. **(D)** Percentage of total Tc-DTPA remaining after 60 min of gamma imaging. *n* = 8-12 animals per group, *P < 0.05, **P < 0.01, ***P < 0.001 compared to air control, using two-way ANOVA.

Figure 2. A ferret model of COPD exhibits abnormal local airway epithelial anatomy and function. (A) Representative µOCT stills of trachea excised from air- or smoke-exposed ferrets. Red line = airway surface liquid (ASL). Yellow line = periciliary layer (PCL). Epi = epithelium. Mu = mucus. **(B)** Representative re-slices of µOCT videos for mucociliary transport (MCT) rate quantification. Yellow arrows represent mucus transport. **(C)** ASL, **(D)** PCL, **(E)** ciliary beat frequency (CBF), and **(F)** MCT rate were quantified for each ferret. *n* = 27 air control and 28 smoke-exposed, *P < 0.05 compared to air control, as assessed by unpaired Mann-Whitney. Data are presented as box-and-whisker (median ± quartiles, using Tukey's method).

Figure 3. Cholinergic stimulation rescues mucus transport in COPD ferret trachea. A-D: ASL **(A)**, PCL **(B)**, CBF **(C)**, and MCT **(D)** were quantified for each

animal. Data is plotted as pre- and post-stimulation pairs by individual animal. *n* = 27 air control and 28 smoke-exposed ferrets, *P < 0.05, ***P < 0.001, ****P < 0.0001 compared to baseline and based on paired Wilcoxon tests.

Figure 4. Smoke-exposed ferrets exhibit a trend toward increased mucus viscosity. (A) Representative H&E and AB/PAS staining of tracheal sections and lung tissue from air control and smoke-exposed ferrets. Black arrows depict submucosal glands. **B-E:** Particle tracking microrheology (PTM) was used to measure ferret tracheal mucus viscosity. **(B)** Representative tracings of the Brownian motion of individual 500-nm particles moving through mucus collected from air- or smoke-exposed ferrets. MSD **(C)** and corresponding effective viscosities over a range of frequencies **(D)** and at 0.6 Hz **(E)** for each group. **(F)** Mucus percent solid content was calculated from measured wet and dry weights. *n* = 12-15 animals per group, *P < 0.05 compared to air control, using unpaired Student's t-test.

Figure 5. Histopathology of normal control, healthy smoker, and COPD human airway tissue. Representative H&E and AB/PAS staining of bronchial sections obtained from non-smoker, healthy smoker, and COPD donors. g = submucosal glands.

Figure 6. Healthy smoker and COPD HBE cells perpetuate mucus abnormalities. (A) Representative tracings of the Brownian motion of individual 1-µm particles moving through normal control, healthy smoker, and COPD mucus. **B-C:** PTM was used to measure mean-squared displacement (MSD) of particles over time **(B)** within mucus

secreted by HBE cells (normal, healthy smoker, COPD), from which effective viscosity **(C)** was calculated. **(D)** Comparison of effective viscosity of each group at 0.6 Hz. **(E)** Mucus percent solids content by weight was calculated for each donor group. **(F)** The relationship between mucus solid content and effective viscosity for each donor. *n* = 1 normal, 3 healthy smoker, 3 COPD donors (with 2-4 samples per donor for PTM, and 6 samples per donor for percent solids), *P<0.05, **P<0.01, ****P<0.0001 compared to COPD using two-way ANOVA (panel B), compared to healthy smoker unless otherwise denoted with two-way ANOVA (panel C), or compared to COPD unless otherwise denoted by one-way ANOVA (panels D-E).

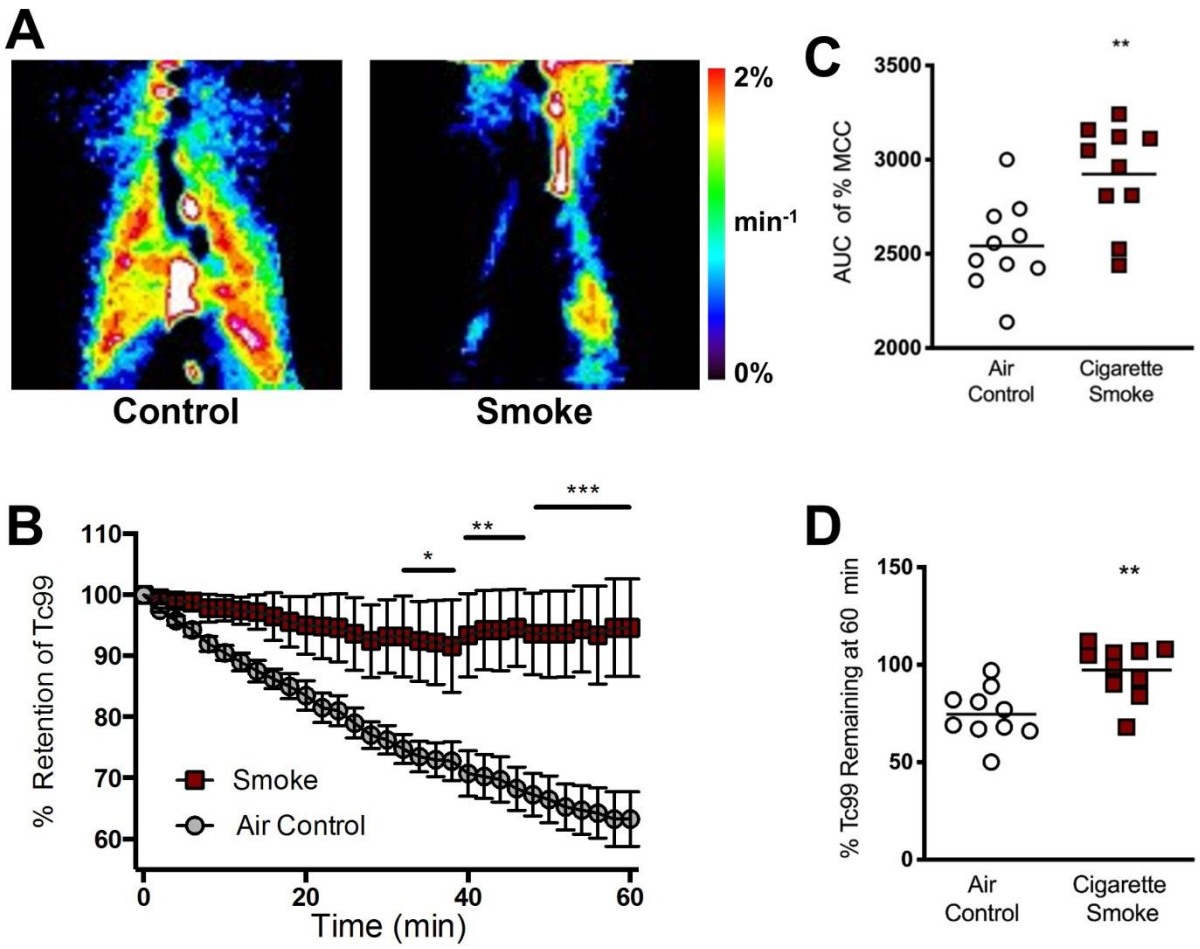
A
2%
min-1
0%
Control
Smoke
C
AUC of % MCC
3500
3000
2500
2000
**
Air Control
Cigarette Smoke
B
% Retention of Tc99
110
100
90
80
70
60
*
**
***
Smoke
Air Control
0
20
40
60
Time (min)
D
% Tc99 Remaining at 60 min
150
100
50
0
**
Air Control
Cigarette Smoke

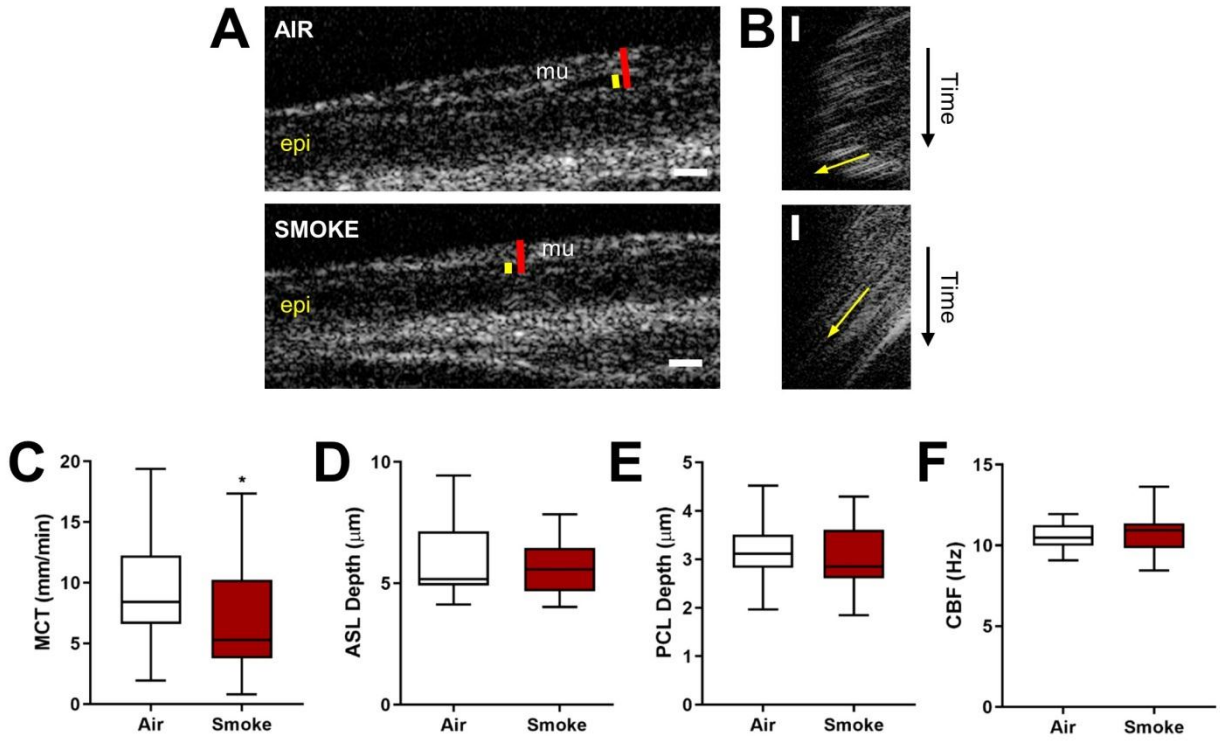
A
AIR
mu
epi
SMOKE
mu
epi
B
I
Time
I
Time
C
MCT (mm/min)
20
15
10
5
0
*
Air
Smoke
D
ASL Depth (μm)
10
5
0
Air
Smoke
E
PCL Depth (μm)
5
4
3
2
1
0
Air
Smoke
F
CBF (Hz)
15
10
5
0
Air
Smoke

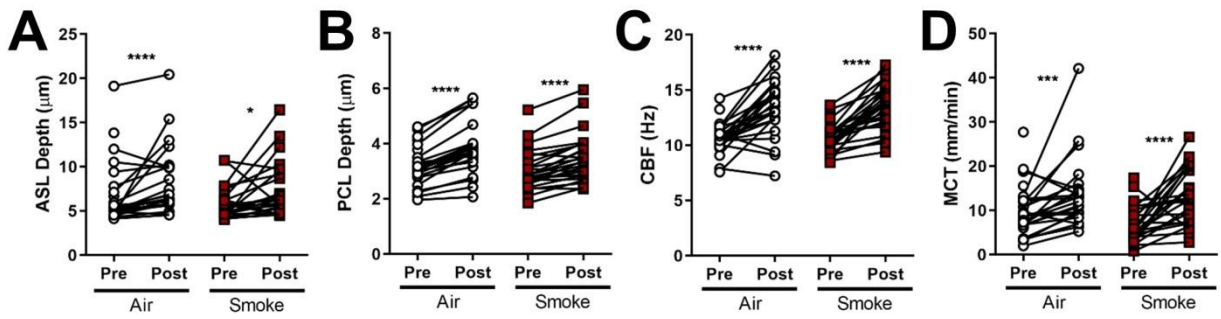
A
ASL Depth (μm)
25
20
15
10
5
0
****
*
Pre
Post
Pre
Post
Air
Smoke
B
PCL Depth (μm)
8
6
4
2
0
****
****
Pre
Post
Pre
Post
Air
Smoke
C
CBF (Hz)
20
15
10
5
0
****
****
Pre
Post
Pre
Post
Air
Smoke
D
MCT (mm/min)
50
40
30
20
10
0
***
****
Pre
Post
Pre
Post
Air
Smoke

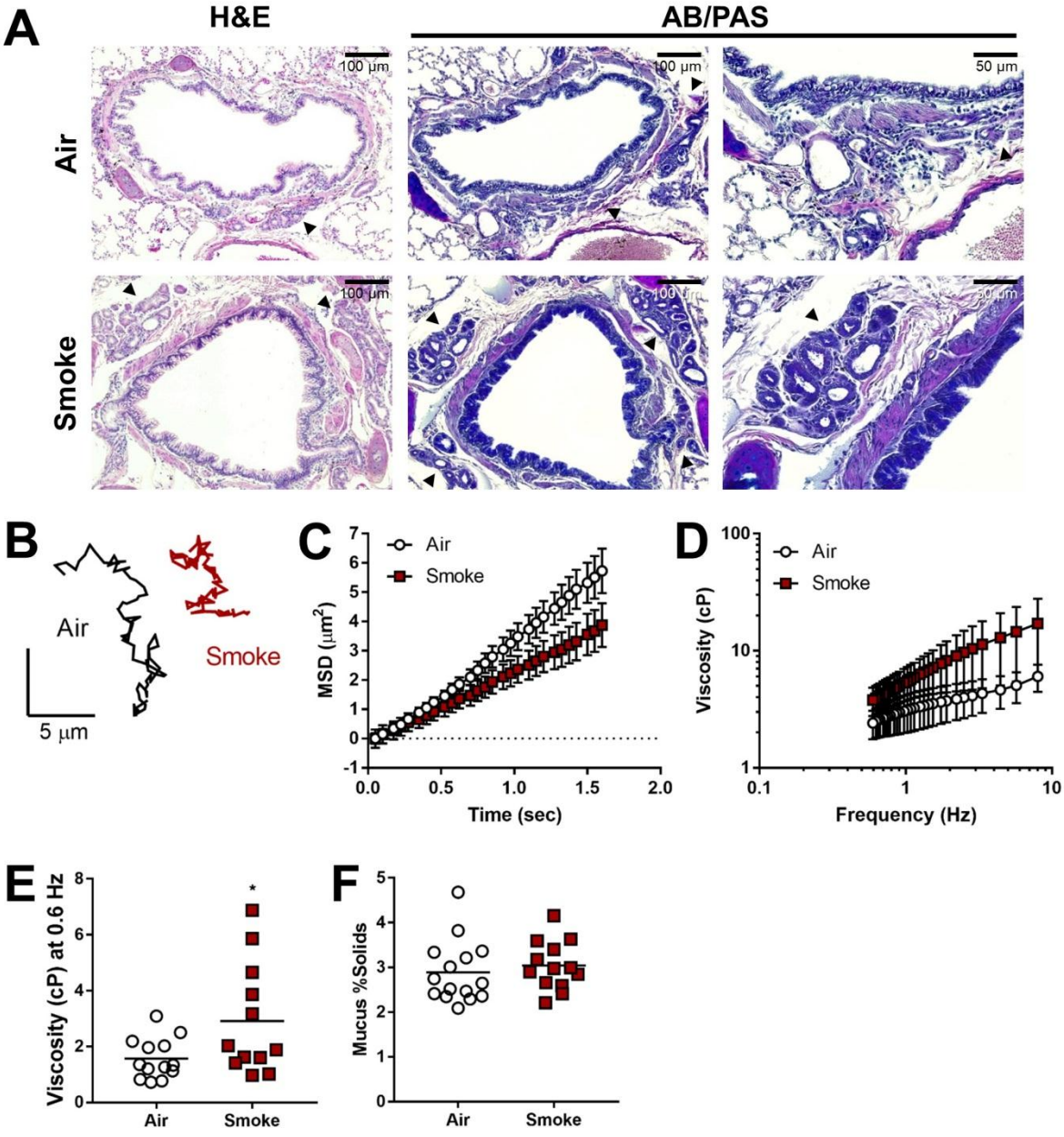
A
H&E
AB/PAS
Air
Smoke
100 µm
50 µm
B
Air
Smoke
5 µm
C
Air
Smoke
MSD (µm²)
Time (sec)
D
Air
Smoke
Viscosity (cP)
Frequency (Hz)
E
Viscosity (cP) at 0.6 Hz
Air
Smoke
F
Mucus %Solids
Air
Smoke

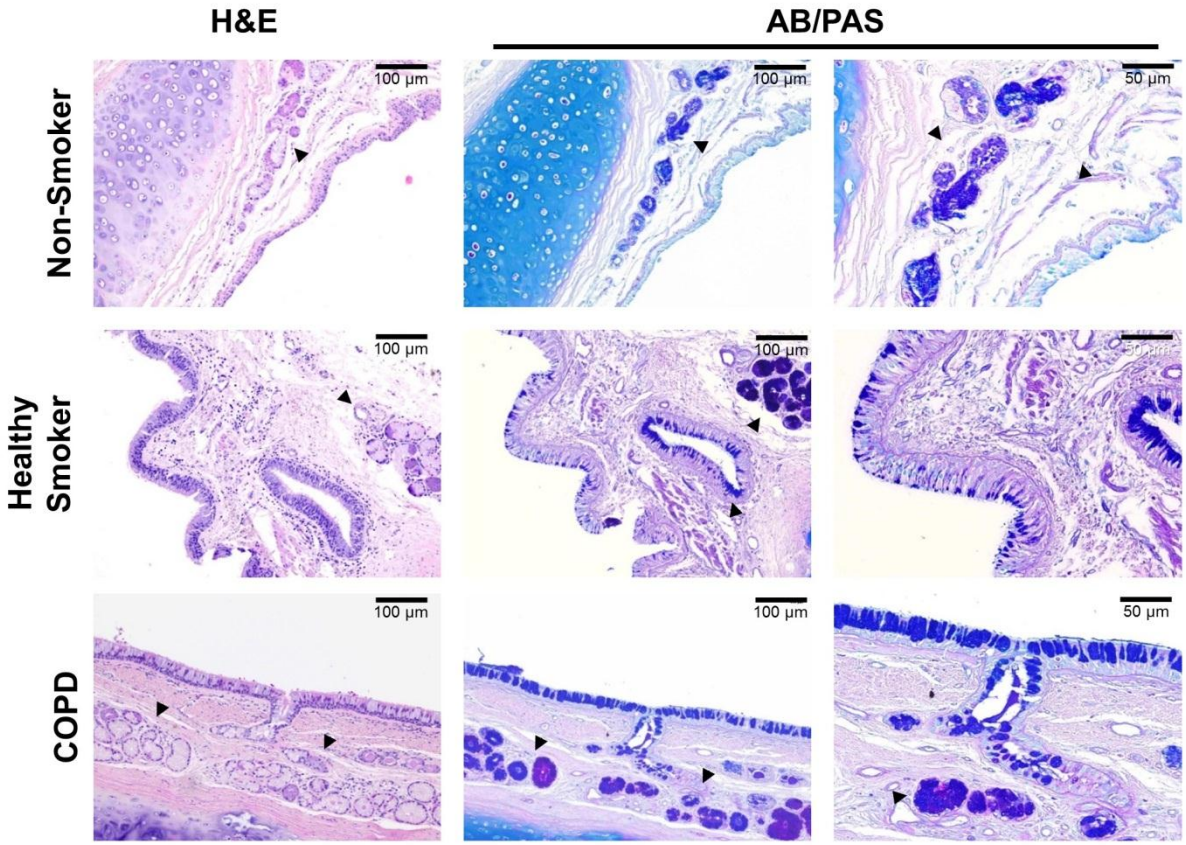
H&E
AB/PAS
Non-Smoker
Healthy Smoker
COPD
100 µm
100 µm
50 µm
100 µm
100 µm
100 µm
100 µm
50 µm

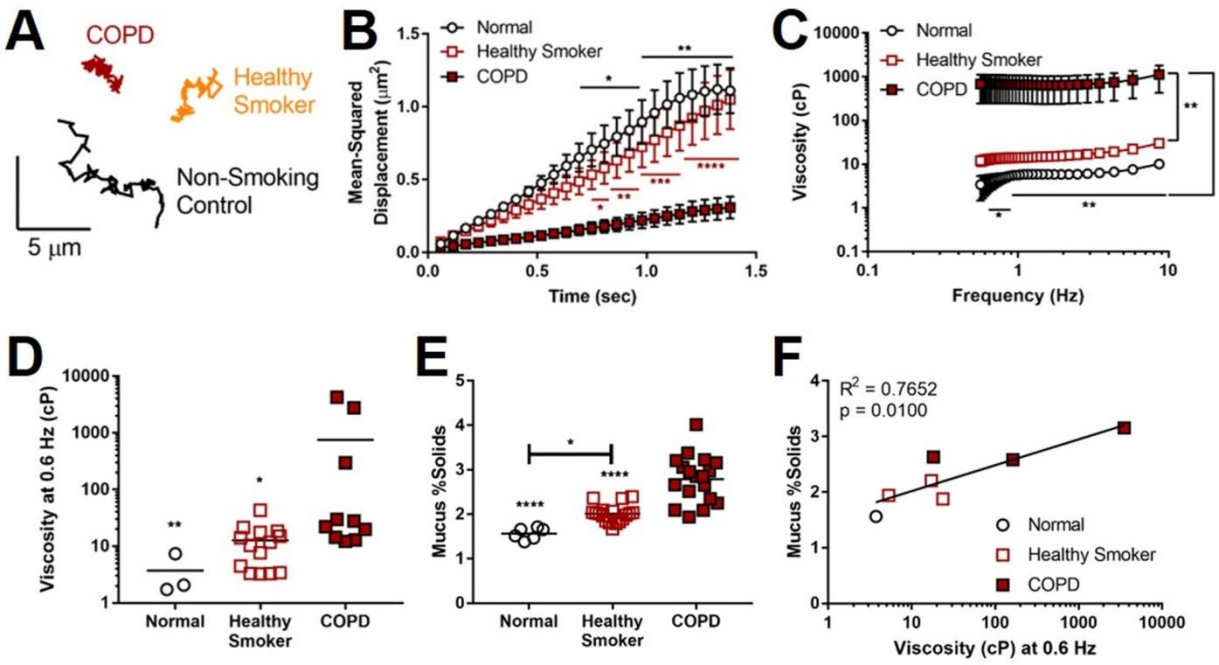
A
COPD
Healthy Smoker
Non-Smoking Control
5 μm
B
Normal
Healthy Smoker
COPD
Mean-Squared Displacement (μm²)
Time (sec)
C
Normal
Healthy Smoker
COPD
Viscosity (cP)
Frequency (Hz)
D
Viscosity at 0.6 Hz (cP)
Normal
Healthy Smoker
COPD
E
Mucus %Solids
Normal
Healthy Smoker
COPD
F
R² = 0.7652
p = 0.0100
Mucus %Solids
Normal
Healthy Smoker
COPD
Viscosity (cP) at 0.6 Hz

Online Data Supplement

Excess mucus viscosity and airway dehydration impact COPD airway clearance

Vivian Y. Lin, Niroop Kaza, Susan E. Birket, Harrison Kim, Lloyd J. Edwards, Jennifer LaFontaine, Linbo Liu, Marina Mazur, Liping Tang, Stephen A. Byzek, Justin Hanes, Guillermo J. Tearney, S. Vamsee Raju, Steven M. Rowe*

Extended Materials and Methods

Smoke exposure

Primary HBE cells were apically exposed to 2% cigarette smoke extract (CSE) [1] or DMSO vehicle (24 hr) prior to imaging. All cigarette smoke was generated from 3R4F cigarettes (University of Kentucky, Lexington, Kentucky, USA).

Standardized anesthesia and intubation protocol

Ferrets (0.6-1.8 kg in weight) were anesthetized with an IACUC-approved formulation of dexmedetomidine (0.4 mg/kg, IM) in combination with ketamine (2.8 mg/kg, IM). Ophthalmic lubricant was applied to the eyes once sedation was achieved. The animals were placed on a heated operating table until recovery. Atipamezole was given as a reversal agent at an equal volume as the dexmedetomidine.

In vivo mucociliary clearance

Sedated ferrets were placed in nose-only restraint tubes similar to the ones used for smoke exposures for administration of ^{99}Tc. Regions of interest (ROI) corresponding to the entire left and right lungs were determined as indicated by concomitant chest radiograph, and counts measured and calculated after correction for radioactive decay. Results were expressed as percentage of radioactivity present in the initial baseline image. Data are plotted as retention of radioactivity vs. time for the whole lung.

Tissue preparation

Connective tissue was removed from excised tracheal and bronchial sections before opening each along the non-cartilaginous tissue for imaging. Samples were incubated at 37°C (5% CO_2) between imaging sessions. All agents were added to the basolateral surface of the trachea (so as not to add exogenous fluid to the apical surface), and stimulants were allowed to incubate for a sufficient duration (30 min) to impart their effects. Indomethacin was used to avoid prostaglandin signaling as a mediator of pharmacologic agents [2], while low-dose carbachol helped stimulate some epithelial secretion for additional mucus transport measurements. Following these imaging treatments, each ferret trachea was then treated with a combination of higher concentration carbachol and phenylephrine, which was necessary to stimulate maximal secretion (5-30 µL collected volume) for subsequent collection and use in mucus-related assays.

Micro-optical coherence tomography (µOCT) imaging

This real-time system provides high-resolution, cross-sectional images of the airway epithelial surface, thereby allowing for simultaneous quantification of airway surface liquid (ASL) depth, periciliary layer (PCL) height, cilia beat frequency (CBF), and mucociliary transport (MCT) rate in a co-localized fashion. Multiple ROI (2-4 per transwell filter or at least 10 per trachea) were imaged to account for variability within individual samples. Cells were imaged at baseline and 24 hr post-exposure.

Particle tracking microrheology (PTM)

Fluorescent beads were imaged using TRITC (500-nm) and GFP (1- µm) channels in the same ROI, and in the same or adjacent plane. 4-5 ROI were imaged per coverslip, with 10-25 individual particles per ROI tracked using ImageJ SpotTracker (NIH); these tracks were then sorted and analyzed using custom MatLab scripts to quantify mean-squared displacement of particles over time, from which effective viscosity can be calculated [3].

Histological staining.

Formalin-fixed human and ferret airway tissues were stained with hemotoxylin and eosin (H&E) or Alcian blue/periodic acid-Schiff (AB/PAS), to assess smoke-induced changes in morphology and mucus-producing structures, respectively.

Statistical analysis.

All groups of data were analyzed using the D'Agostino-Pearson normality test to determine whether a parametric or non-parametric test should be used. Results for airway microanatomy and viscoelasticity metrics between control and smoke-exposed tissues over time were assessed by two-way ANOVA, and those between control and COPD or smoke-exposed groups were compared using unpaired Mann-Whitney or t-test. Wilcoxon was used to compare paired measures pre- and post-stimulation within each exposure group. Correlations between metrics were calculated using linear or semi-log regression methods. A univariate model was performed to assess for effects on mean MCT. A linear mixed model for repeated measures analysis was used to model MCT as a repeated measure (technical and biological replicates) using

previously published statistical methods [4, 5], and predictors included time effects, cohort effects, sex effects, smoking effects, and the potential for interaction among them. A separate linear mixed model was used to assess the relationship between MCT and mean ASL, mean PCL, and mean CBF as independent variables along with time category, smoking status, cohort, and sex. Random effects included intercept and repeated measures at baseline, or random intercept only. Unstructured random effects covariance matrix was used for each analysis. The final models omitted interaction terms between predictor variables and time or cohort, as these were not significant and did not alter conclusions. R^2 were estimated by previous methods [6].

Supplemental Tables

Table S1. Univariate linear regression analysis for mean MCT in steady-state conditions. By ferret (N=54).

Predictor	β	P-value	R^2
Smoke	-3.09	**< 0.028**	0.089
CBF	1.34	**< 0.007**	0.129
PCL	0.530	0.608	0.005
ASL	-0.40	0.114	0.047
Female	-0.22	0.879	0.000

Table S2. Tissue donor demographics.

	Non-Smoker (n = 3)	**Healthy Smoker** (n = 6)	**COPD** (n = 3)
Gender	Female (1) Male (2)	Male (6)	Female (2) Male (1)
Age (years)	44 ± 19.8	44.5 ± 9.8	51.3 ± 9.1
Race	White (2) Black (1)	White (6)	White (1) Black (2)
Donors with emphysema	0	0	1
Smoking history (Pack-years)	N/A	34.3 ± 17.5	36.7 ± 29.3

Supplemental Figure Legends

Figure S1. Deposition of Tc^{99}-DTPA in ferret tissues. (A) Representative uncorrected images of Tc^{99}-DTPA deposition in the lungs acquired at baseline (Time 0). **(B)** Total deposition of radiolabel at Time 0 was quantified before assessment of clearance. **(C)** Systemic absorption of Tc^{99}-DTPA as monitored by uptake into forearm muscles.

Figure S2. Schematic of experimental protocol for ferret trachea. Upon euthanization, the trachea was removed from each animal and immediately dissected for µOCT imaging, followed by cholinergic stimulation of mucus secretion for assessment of mucus properties such as microrheology and percent solids by weight. Thick borders indicate endpoint collection throughout the protocol. Capitalized words indicate key timepoints for endpoints. Abbreviations: µOCT = micro-optical coherence tomography, PTM = particle tracking microrheology.

Figure S3. Distribution of µOCT-quantified airway epithelial function by region of interest (ROI). µOCT was used to measure **(A)** ASL depth, **(B)** PCL height, **(C)** CBF, and **(D)** MCT rate at multiple ROI per ferret trachea, to account for the local microenvironment. Data is presented as box-and-whisker (Tukey method). n = 1078 videos.

Figure S4. Cigarette smoke exposure reduces MCT in primary HBE cells. (A) Representative µOCT stills of primary HBE cells after 24-hour apical treatment with 2% cigarette smoke extract (CSE) or DMSO control. Red line = ASL. Yellow line = PCL. **B-**

C: Quantification of *in vitro* ASL **(B)** and MCT **(C)** following exposure. *n* = 10 ROI, **p < 0.01, ***p < 0.001 compared to vehicle control, as determined by unpaired Mann-Whitney (ASL) and t-test (MCT).

References in Online Supplement

1. Raju SV, Lin VY, Liu L, McNicholas CM, Karki S, Sloane PA, Tang L, Jackson PL, Wang W, Wilson L, Macon KJ, Mazur M, Kappes JC, DeLucas LJ, Barnes S, Kirk K, Tearney GJ, Rowe SM. The Cystic Fibrosis Transmembrane Conductance Regulator Potentiator Ivacaftor Augments Mucociliary Clearance Abrogating Cystic Fibrosis Transmembrane Conductance Regulator Inhibition by Cigarette Smoke. *Am J Respir Cell Mol Biol* 2017: 56(1): 99-108.
2. Joo NS, Jeong JH, Cho HJ, Wine JJ. Marked increases in mucociliary clearance produced by synergistic secretory agonists or inhibition of the epithelial sodium channel. *Sci Rep* 2016: 6: 36806.
3. Chu KK, Mojahed D, Fernandez CM, Li Y, Liu L, Wilsterman EJ, Diephuis B, Birket SE, Bowers H, Martin Solomon G, Schuster BS, Hanes J, Rowe SM, Tearney GJ. Particle-Tracking Microrheology Using Micro-Optical Coherence Tomography. *Biophys J* 2016: 111(5): 1053-1063.
4. Laird NM, Ware JH. Random-effects models for longitudinal data. *Biometrics* 1982: 38(4): 963-974.
5. Edwards LJ. Modern statistical techniques for the analysis of longitudinal data in biomedical research. *Pediatr Pulmonol* 2000: 30(4): 330-344.
6. Edwards LJ, Muller KE, Wolfinger RD, Qaqish BF, Schabenberger O. An R2 statistic for fixed effects in the linear mixed model. *Stat Med* 2008: 27(29): 6137-6157.

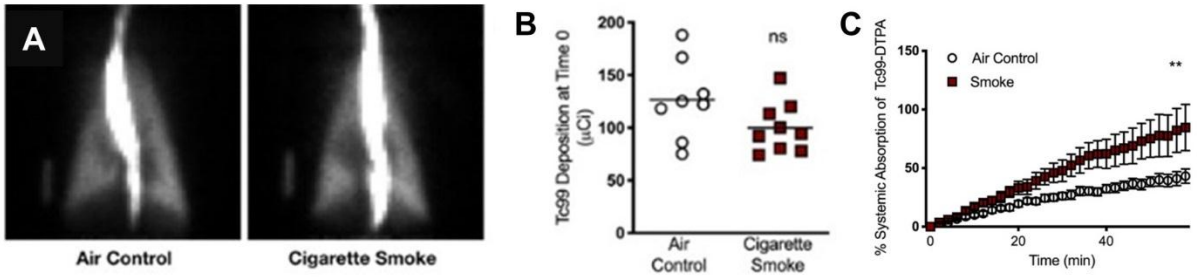
A
Air Control
Cigarette Smoke
B
Tc99 Deposition at Time 0 (μCi)
200
150
100
50
0
ns
Air Control
Cigarette Smoke
C
% Systemic Absorption of Tc99-DTPA
150
100
50
0
Air Control
Smoke
**
0
20
40
Time (min)

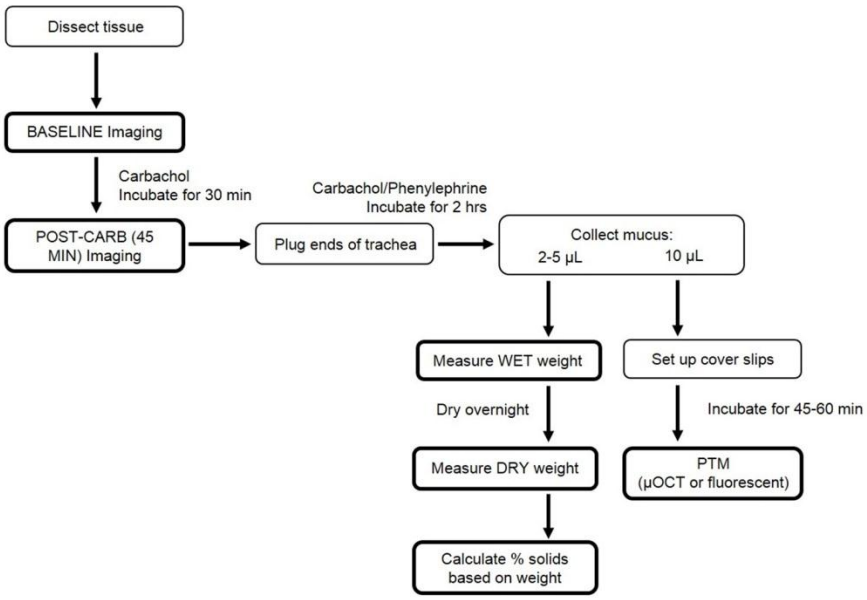
Dissect tissue
BASELINE Imaging
Carbachol
Incubate for 30 min
POST-CARB (45 MIN) Imaging
Carbachol/Phenylephrine
Incubate for 2 hrs
Plug ends of trachea
Collect mucus:
2-5 µL
10 µL
Measure WET weight
Dry overnight
Measure DRY weight
Calculate % solids based on weight
Set up cover slips
Incubate for 45-60 min
PTM
(µOCT or fluorescent)

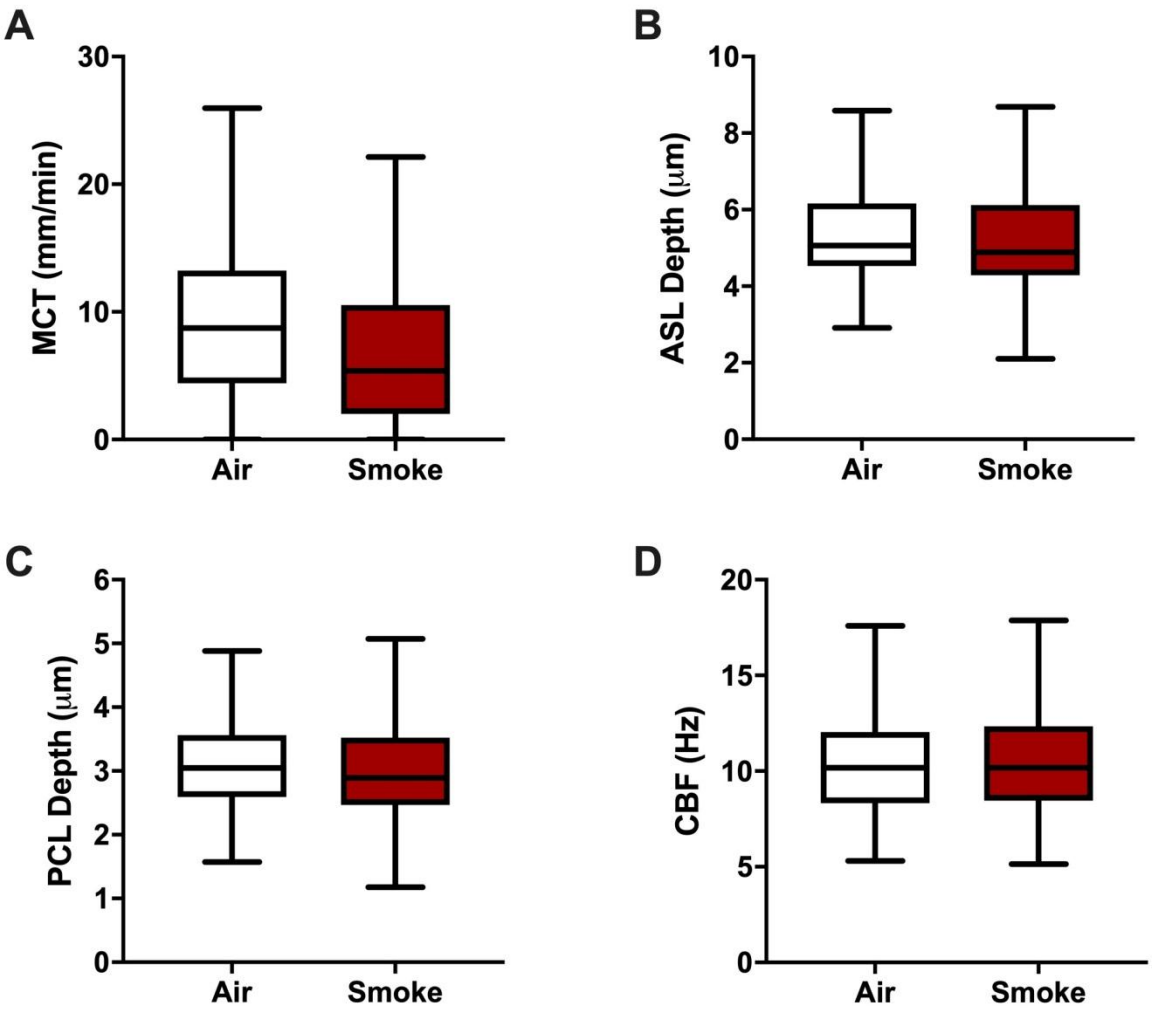
A
MCT (mm/min)
30
20
10
0
Air
Smoke
B
ASL Depth (μm)
10
8
6
4
2
0
Air
Smoke
C
PCL Depth (μm)
6
5
4
3
2
1
0
Air
Smoke
D
CBF (Hz)
20
15
10
5
0
Air
Smoke

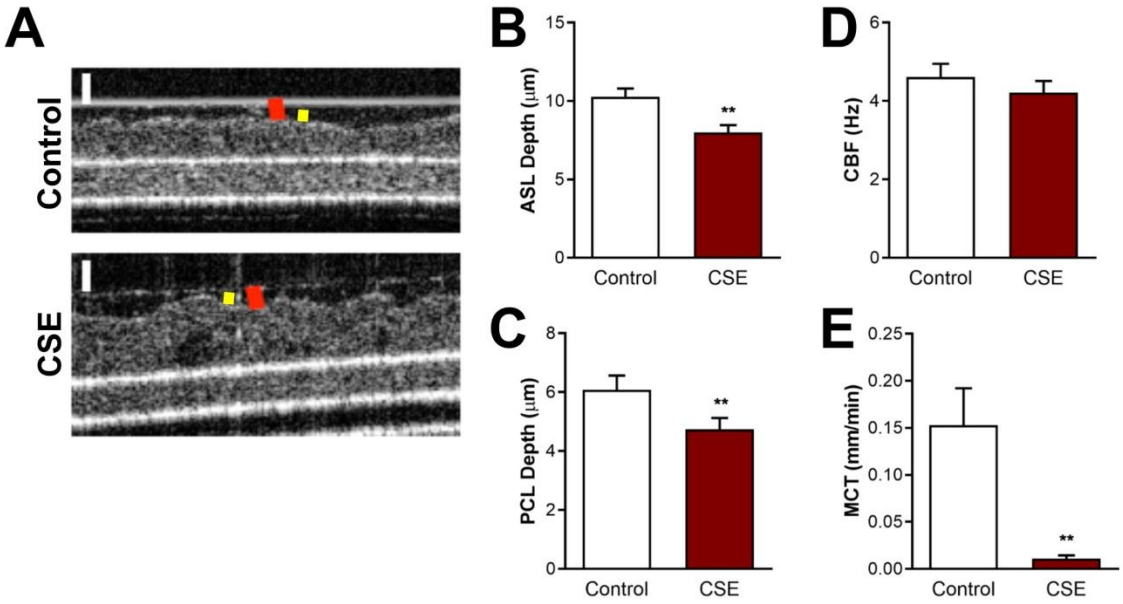
A
Control
CSE
B
ASL Depth (μm)
15
10
5
0
**
Control
CSE
D
CBF (Hz)
6
4
2
0
Control
CSE
C
PCL Depth (μm)
8
6
4
2
0
**
Control
CSE
E
MCT (mm/min)
0.25
0.20
0.15
0.10
0.05
0.00
**
Control
CSE